Asian Herpetological Research 2016, 7(2): 75–86
DOI: 10.16373/j.cnki.ahr.150040

ORIGINAL ARTICLE

Genetic Diversity and Population Structure for the Conservation of Giant Spiny Frog (*Quasipaa spinosa*) Using Microsatellite Loci and Mitochondrial DNA

Danna YU[1], Rongquan ZHENG[1,2*], Qinfang LU[1], Guang YANG[2,3], Yao FU[1] and Yun ZHANG[1]

[1] *Institute of Ecology, Zhejiang Normal University, Jinhua* 321004, *Zhejiang, China*
[2] *Key Lab of Wildlife Biotechnology and Conservation and Utilization of Zhejiang Province, Jinhua, Zhejiang* 321004, *China*
[3] *Jiangsu Key Laboratory for Biodiversity and Biotechnology, College of Life Sciences, Nanjing Normal University, Nanjing* 210046, *Jiangsu, China*

Abstract The giant spiny frog (*Quasipaa spinosa*) is an endangered species with a relatively small distribution limited to southern China and Northern Vietnam. This species is becoming increasingly threatened because of over-exploitation and habitat degradation. This study provides data on the genetic diversity and population genetic structure of the giant spiny frog to facilitate the further development of effective conservation recommendations for this economically important but threatened species. We examined 10 species-specific microsatellite loci and Cyt *b* genes (562 bp) collected from 13 wild populations across the entire range of this species. Results of 10 microsatellite loci analysis showed a generally high level of genetic diversity. Moreover, the genetic differentiation among all 12 populations was moderate to large (overall $F_{ST} = 0.1057$). A total of 51 haplotypes were identified for Cyt *b*, which suggests high haplotype nucleotide diversities. Phylogeographic and population structure analyses using both DNA markers suggested that the wild giant spiny frog can be divided into four distinct major clades, i.e., Northern Vietnam, Western China, Central China, and Eastern China. The clades with significant genetic divergence are reproductively isolated, as evidenced by a high number of private alleles and strong incidence of failed amplification in microsatellite loci. Our research, coupled with other studies, suggests that *Q. spinosa* might be a species complex within which no detectable morphological variation has been revealed. The four phylogenetic clades and some subclades with distinct geographical distribution should be regarded as independent management units for conservation purposes.

Keywords Cyt *b*, Conservation, Giant spiny frog, Microsatellite, Phylogeography, *Quasipaa spinosa*

1. Introduction

The giant spiny frog (*Quasipaa spinosa*) is known for the keratinized skin-spines on its chest and the development of hypertrophied forearms as a secondary sex organ in males during the breeding season (Yu *et al.*, 2010). This species inhabits rocky streams in evergreen forests and open fields on mountains 500 m to 1,500 m above sea level (Zhao, 1998). In Chinese markets, the giant spiny frog is especially valued for its medicinal and nutritional properties, particularly for the high amount of protein contained in its muscles (Ye *et al.*, 1993; Zhao, 1998). In addition to harvesting, the habitats of *Q. spinosa* were destroyed by pollution from upland agriculture and dam and hydropower projects (Chan *et al.*, 2014). Commercial over-exploitation and habitat destruction caused the wild population of this species significantly decline, both in number and distribution (Zhao, 1998).

In 2001, the International Union for the Conservation of Nature (IUCN) Red List registered this species as vulnerable (A2abc) and estimated that over the last three

* Corresponding author: Dr. Rongquan ZHENG, from Zhejiang Normal University, with his research focusing on amphibian molecular ecology. E-mail: zhengrq@zjnu.cn
Received: 10 November 2015 Accepted: 25 February 2016

generations (approximately 15 years), the wild population had decreased by 30% (Lau *et al.*, 2004; Zhao, 1998). Despite the initiation of domestication and artificial breeding programs in the 1980s, the culture of giant spiny frog remains relatively small in scale because of low fertilization and hatching rates, disease, high overwinter mortality, and inbreeding depression (Chan *et al.*, 2014; Liang *et al.*, 2013). Farming of giant spiny frog mainly depends on the natural supply of tadpoles or adults (Chan *et al.*, 2014; Liang *et al.*, 2013).

Recent phylogenetic study suggested that *Q. spinosa* may be a cryptic species complex (Che *et al.*, 2009; Ye *et al.*, 2013). However, most frog farms are using frogs from different geographical populations to produce offspring without a detailed record of genetic and performance data (Chan *et al.*, 2014). This practice poses a risk of genetic contamination and a threat of pathogen transmission. Escapees from aquaculture and translocation or even deliberate releases of tadpoles, if not sourced from the same location, have the potential to interbreed with wild frog, thus possibly modifying the genetic structure of wild populations. Interbreeding of *Q. spinosa* from genetically distinct populations can potentially reduce the fitness and viability of a species, which then becomes increasingly vulnerable to extinction over time (Borrell *et al.*, 2011; Miller *et al.*, 2011). These issues require knowledge of the genetic structure of the species; such knowledge is important for the conservation of indigenous genetic diversity (Chan *et al.*, 2014; Miller *et al.*, 2011).

Information on the intra-specific genetic diversity and relationships among the wild populations of this endangered species remains lacking. Che *et al*. (2009) suggested that the populations currently under *Q. spinosa* likely belong to at least three independent evolutionary lineages, but only seven specimens from four localities were used as bases from which to infer phylogenetic relationships. The sample sizes are too small to reflect the genetic diversity and relationships among the populations of *Q. spinosa*. Ye *et al*. (2013) also supported that *Q. spinosa* is a species complex, rather than a single species, on the basis of 12S rRNA and 16S rRNA genes. However, the use of mtDNA alone is insufficient to reflect the quantification and distribution of genetic variation (Dupuis *et al.*, 2012).

In this study, we analyzed data from microsatellite (10 microsatellite loci) and mitochondrial (Cyt *b* gene) loci collected from *Q. spinosa* along the entire range of this species to evaluate the phylogeography and population genetics of *Q. spinosa*, as well as to provide genetic information for further developing effective conservation recommendations to protect this economically important but threatened species.

2. Materials and Methods

2.1 Sample collection and DNA extraction Two hundred and five samples were collected from 13 localities during 2006 and 2007, in China and Vietnam, namely the province (city); Anhui (Huangshan), Fujian (Jianyang, Wuyishan), Hunan (Pingjiang), Guangdong (Yangshan), Guangxi (Longsheng, Yongfu), Jiangxi (Jinggangshan), Yunnan (Pingbian), Zhejiang (Jinhua, Lishui) and Northern Vietnam. Specific spatial details of the collection sites are given in Fig. 1 and Table 1. The collection sites were almostly covered the entire geographical range of giant spiny frog (Frost *et al.*, 2006). Some samples were released after obtaining their toe clips.

Muscle or toe clips samples were stored in 95% or 100% ethanol, or frozen at –80°C. The study protocol was reviewed and approved by the Committee of Animal Research Ethics of Zhejiang Normal University. DNA was extracted using the standard phenol-chloroform procedure (Sambrook *et al.*, 1989).

Table 1 Sampling information of giant spiny frog. Geographic sampling localities with their coordinates, number of sample sizes for sample sizes of Cyt *b* (N) and number of sample sizes for microsatellite (n) are shown.

Geographic locality (ab.)	N/n	Coordinates
Northern Vietnam (VT)	5/0	E 104.33º, N 21.60º
Pingbian, Yunnan (PB)	5/9	E 103.60º , N 22.81º
Yongfu, Guangxi (YF)	14/16	E 109.98º, N 24.98º
Longsheng, Guangxi (LH)	13/27	E 109.98°, N 25.82°
Yangshan, Guangdong (YS)	4/17	E 112.63°, N 24.48°
Pingjiang, Hunan (PJ)	16/23	E 113.58°, N 28.72°
Jinggangshan, Jiangxi (JG)	6/24	E 114.10°, N 26.34°
Xingan, Jiangxi (XG)	5/10	E 115.60º, N 27.77º
Wuyishan, Fujian (WY)	8/19	E 118.01°, N 27.27°
Jianyang, Fujian (JY)	5/13	E 118.60°, N 27.41°
Lishui, Zhejiang (LS)	11/18	E 119.54°, N 28.27°
Jinhua, Zhejiang (JH)	15/14	E 119.62º, N 29.11º
Huangshan, Anhui (HS)	15/15	E 118.57º, N 30.07º
Total	122/205	

2.2 Microsatellite genotyping and analysis Among the 15 developed and characterized species-specific genetic markers, 10 proved to be polymorphic and were used in this study (Table S1) (Zheng *et al.*, 2009). Microsatellite genotyping was performed on all individuals from 13 localities, but the Northern Vietnam population could not be included in the analyses because all individuals and loci failed in the amplification. The DNA of Northern Vietnam individuals was extracted several times using a standard phenol-chloroform procedure and DNeasy Tissue Kit (Qiagen), and the electrophoretic band (0.8% agarose) was significantly brighter than 25 ng standard for DNA quantification. Amplification was performed by gradient temperature polymerase chain reaction (PCR) (44°C to 68°C), but none of the loci can be successfully amplified.

Amplification was performed in a reaction volume of 25 μL with approximately 0.5 μL genomic DNA, 15.88 μL of ddH_2O, 2.5 μL of 10× PCR buffer (Mg^{2+} free), 1 μL (10 pmol) of each primer, 2 μL $MgCl_2$ (25mM), 2 μL dNTP Mixture (2.5mM), and 0.125 μL of TaKaRa *Taq* (5 U/μL). Following the dye label incorporation procedures from Schuelke (Schuelke, 2000), the forward primer 5′ was appended with a 19 bp M13 sequence (CACGACGTTGTAAAACGAC) and employed at 0.4 μm, whereas the reverse primer used a fluorescent-labeled "M13" primer and employed at 0.4 pmol [either IRD700 or IRD 800(LI-COR)]. The PCR thermocycler profile was as follows: 95°C for 5 min followed by 35 cycles at 95 °C for 30 s, and annealing temperature for 30 s (Table S1); 72 °C for 30 s; and a final extension step at 72°C for 8 min. The amplified products were analyzed on a LI-COR4300 automated DNA sequencer using 6.5% denaturing polyacrylamide gels with appropriately labeled 50 bp to 350 bp internal size standard. The gel images were analyzed using the LI-COR SAGA software.

The number of alleles per locus (*N*a), heterozygosity (*H*), Allelic frequencies, polymorphic information content (*PIC*), as well as observed (H_O) and expected (H_E) heterozygosities were calculated using Cervus 2.0 software (Marshall *et al.*, 1998). Unique alleles, defined as an allele found in only one of the populations, were detected using GDA (Lewis and Zaykin, 2000). The potential deviations from Hardy–Weinberg equilibrium (HWE) and linkage disequilibrium (LD) were estimated using Arlequin version 2.0 and modified Fisher's exact test (Guo and Thompson, 1992; Schneider *et al.*, 2000). Results of the multiple comparisons were adjusted using Bonferroni correction.

The population genetic differentiation was quantified using the F_{ST}-estimator of Weir and Cockerham (Weir and Cockerham, 1984). A Bayesian clustering method was used to organize the dataset and to assign individuals to inferred clusters by using the STRUCTURE software package (Pritchard *et al.*, 2000). Individuals were placed into K clusters using the model-based algorithm, with K chosen in advance. A total of 12 independent runs of K=1 to K=12 were performed at 1,000,000 Markov Chain Monte Carlo (MCMC) repetitions with a 100,000 burn-in period assumed with allele frequencies and combinations without prior information (Du *et al.*, 2012; Pritchard *et al.*, 2000). The log likelihood was used to choose the most likely value for K. The posterior probability K [P(K|X)] was then calculated. Statistic DK, which is the second-order rate of the log probability change of the data between successive values of K, was also estimated (Evanno *et al.*, 2005). The method successfully detected the appropriate number of clusters using multilocus genotype data under a number of gene exchange models. Given that DK could not be evaluated when K = 1, we explored the probability of the K=2 to K=12 on the basis of the above results.

Partitioning genetic diversity through analysis of molecular variance (AMOVA) was performed using ARLEQUIN version 2.0 on the basis of microsatellite data (Schneider *et al.*, 2000). In AMOVA, the total variance was divided into variance among groups, among populations within groups, among individuals within populations, and within individuals.

2.3 Mitochondrial DNA amplification and analysis The Cyt *b* gene was amplified with primers CB-10933 (5′-TAT GTT CTA CCA TGA GGA CAA ATA TC-3′) (Simon *et al.*, 1994) and modified CytbC (5′-CTA CTG GTT GTC CTC CGA TTC ATG T-3′) (Bossuyt and Milinkovitch, 2000). Amplification was performed in a reaction volume of 50 μL that contained approximately 100 ng of template DNA, 2.5 mM $MgCl_2$, 2.0 mM 10×PCR buffer, 0.4 μM of the forward and reverse primers, 0.2 mM of each dNTP, and 1 U rTaq polymerase (TaKaRa, Dalian, China). The PCR thermocycler profile was as follows: 94 °C for 2 min, followed by 35 cycles at 94 °C for 45 s, 56 °C for 45 s, and 72 °C for 1 min; and a final extension step at 72 °C for 10 min. The PCR products were purified using Wizard PCR Preps DNA purification kit (Promega, Beijing, China). Each fragment was sequenced with an ABI automated DNA sequencer in both directions by using the PCR primers.

All sequences were checked with BioEdit software (North Carolina State University) and by visual

inspection. The sequences were then imported into Clustal X (Thompson *et al.*, 1997) for alignment. Genetic diversities for all sampling regions or populations were estimated using haplotype (h) and nucleotide diversities (π), as implemented in DnaSP version 4.0 (Rozas *et al.*, 2003). Sequence divergences between haplotypes and populations were calculated using Arlequin 2.0 (Schneider *et al.*, 2000). Pairwise K2P (Kimura 2-parameter) distances and diagnostic sites for Cyt *b* gene sequences were calculated in MEGA 5.0 to evaluate the intrapopulation and interpopulation divergence of *Q. spinosa* (Tamura *et al.*, 2007). The phylogenetic relationship among haplotypes was reconstructed using maximum likelihood (ML) heuristic search methods through by PAUP*4.0 (Swofford, 2002). The robustness of these analyses was assessed using non-parametric bootstrap replications by PAUP*4.0 with 100 replications

ML analyses were performed with the general time-reversible (GTR+I+G) model of DNA evolution, which has the shape parameter of a gamma distribution (G) (Posada and Crandall, 1998; Swofford, 2002). The GTR+I+G model was identified as the best-fitting model under the Akaike information criterion as implemented in Modeltest 3.7 (Posada and Crandall, 1998). In the Bayesian analysis, we used MrBayes 3.1.2 under the GTR+I+G model (Huelsenbeck and Ronquist, 2001). Posterior distributions were determined by MCMC analysis with one cold chain and three heated chains run for 10 million generations with random starting trees. Every 100th tree was sampled. Bayesian analyses were repeated twice, and the same topology was always retrieved. According to the likelihood plots, lnl values stabilized with 10,000 generations. Thus, the first 100,000 generations were discarded as burn-in. Meanwhile, Bayesian posterior probabilities were calculated according to the remaining set of trees. The rice frog (*Fejervarya limnocharis*) was chosen as the outgroup for all phylogenetic reconstructions (Che *et al.*, 2009; Liu *et al.*, 2005).

To assess the most probable population configuration and geographical subdivision, hierarchical AMOVA was performed using Arlequin 2.0 (Schneider *et al.*, 2000). The populations were grouped according to different geographical distinctions. Genetic differentiation among samples from different geographic origins was assessed by comparing the average number of pairwise differences between populations (PiXY), the average number of pairwise differences within populations (PiX and PiY), and the corrected average pairwise difference (PiXY_(PiX+PiY)/2). Distances and standard error were calculated using Arlequin 2.0 with 1000 bootstrap replicates (Schneider *et al.*, 2000).

3. Results

3.1 Microsatellite DNA analysis

Genetic variation: All 10 microsatellite loci in the 12 populations showed high genetic polymorphism (Tables S1–S2). However, individuals from Northern Vietnam were either non-functional (not amplifying after repeated attempts) or poorly amplified (the electrophoretic bands of PCR products were dispersed). A total of 339 different alleles were detected in 205 individuals from 12 populations. The allele sizes at individual loci varied between 12 bp (for locus Psp7) and 92 bp (for locus Psp10). Examination of genotyping errors using MicroChecker revealed no evidence of large allele dropout or stutter-band scoring at any of the 10 loci. The mean number of alleles varied from 6.3 to 15.1. The mean *PIC* for the 12 populations ranged between 0.63 and 0.88. Within all populations, the H_O (0.49–0.72) was lower than H_E (0.69–0.91) (Table S2). The 12 populations showed very high gene diversity (mean *H*e=0.82). Among the populations, the gene diversities of XG (*H*e=0.90) and WY (*H*e=0.91) were higher than those of other populations. Deviation from HWE and linkage disequilibrium (LD) was also evaluated in all 12 populations. Out of 120 loci (12 populations multiplied by 10 loci), 65 showed deviation from HWE ($P < 0.05$; Table S2). All 10 microsatellites were not in LD ($P > 0.05$) for each pair of loci across all samples.

Genetic structure and gene flow: After Bonferroni correction, some multi-loci F_{ST} values were small, but all values were significant at $P < 0.05$ (Table 2). All of the F_{ST} values, except for five lower than 0.05, fell between 0.05 and 0.25, indicating that a moderate or large differentiation existed in the populations (Wright, 1978). The average of F_{ST} of all loci was 0.1057. The PJ and HS populations had the largest amount of differentiation at 0.2095.

The clustering method revealed that ΔK_{max} was 3.02 and peaked at K = 3. The highest posterior probability (ln Pr (X|K) = –4443.6) of the 20 runs for K = 3 was presented along with color-coded probabilities of individuals belonging to a cluster (Figure 1). The highly non-random association of colors showed three distinct genetic cluster groups among the sampling localities. The cluster groups are the Western China, Central China, and Eastern China clusters. The cluster names

refer to the sample range. The Western China cluster comprised alleles from three populations sampled from Pingbian (PB) of YUNNAN Province, Yangshan (YS) of Guangdong Province, and Longsheng (LH) of Guangxi Zhuang Autonomous Region. The Central China cluster comprised alleles from populations at Yongfu (YF) of Guangxi Zhuang Autonomous Region, Pingjiang (PJ) of Hunan Province, Jinggangshan (JG) and Xingan (XG) of Jiangxi Province, and Wuyishan (WY) of Fujian Province. The eastern China cluster comprised alleles from populations at Jianyang (JY) of Fujian Province, Lishui (LS) and Jinhua (JH) of Zhejiang Province, and Huangshan (HS) of Anhui Province.

A total of 118 unique alleles were detected among the three clusters. The Central China cluster possessed the highest number of unique alleles (57.63%), followed by Western China (23.73%) and Eastern China (18.64%) (Table S3). The cluster groups were also analyzed using hierarchical AMOVA method, which revealed the following statistical significant ($P < 0.001$) substructure: 66.01% of the total genetic variations was observed among the individuals, 1.95% among the groups, 9.46% among populations within the groups, and 22.58% among individuals within groups (Table 3).

3.2 Mitochondrial DNA analysis

Sequence variation and genetic distance: A total of 218 variable (38.79%) sites and 211 parsimony-informative (37.54%) sites were found in the 562-bp Cyt *b* fragments.

Table 2 Pair-wise F_{ST} between the twelve populations estimated from the ten microsatellite loci.

	HS	JH	LS	JY	PJ	XG	WY	JG	YS	LH	YF
HS											
JH	0.2052										
LS	0.1942	0.1299									
JY	0.1673	0.1268	0.0784								
PJ	0.2095	0.1758	0.1310	0.1306							
XG	0.1571	0.1295	0.0808	0.0898	0.0891						
WY	0.1187	0.1213	0.0909	0.0515	0.0942	0.0379					
JG	0.1482	0.1414	0.1118	0.1001	0.1254	0.0937	0.0636				
YS	0.1461	0.1153	0.0669	0.0726	0.1005	0.0615	0.0494	0.0603			
LH	0.1623	0.1328	0.1167	0.1082	0.1274	0.0937	0.0681	0.0848	0.0847		
YF	0.1616	0.1488	0.1313	0.1066	0.1396	0.0902	0.0695	0.1002	0.0882	0.0287	
PB	0.1368	0.1123	0.0904	0.0881	0.1097	0.0686	0.0359	0.0604	0.0529	0.0431	0.0697

Table 3 Nested Analysis of Molecular Variance (AMOVA) indicating partitioning of genetic diversity.

Source of Variation	*d.f.*	Sum of Squares	Variance Components	Percentage of Variation
Among groups	2	66.169	0.090Va	1.95*
Among populations within groups	9	176.139	0.436 Vb	9.46*
Among individuals within populations	193	987.793	1.040 Vc	22.58*
Within individuals	205	623.000	3.039 Vd	66.01*
Total	409	1853.100	4.604	

*All indices are highly significant; the probability (P) of obtaining a more extreme component estimate by chance alone = <0.001 (using 1000 randomizations).

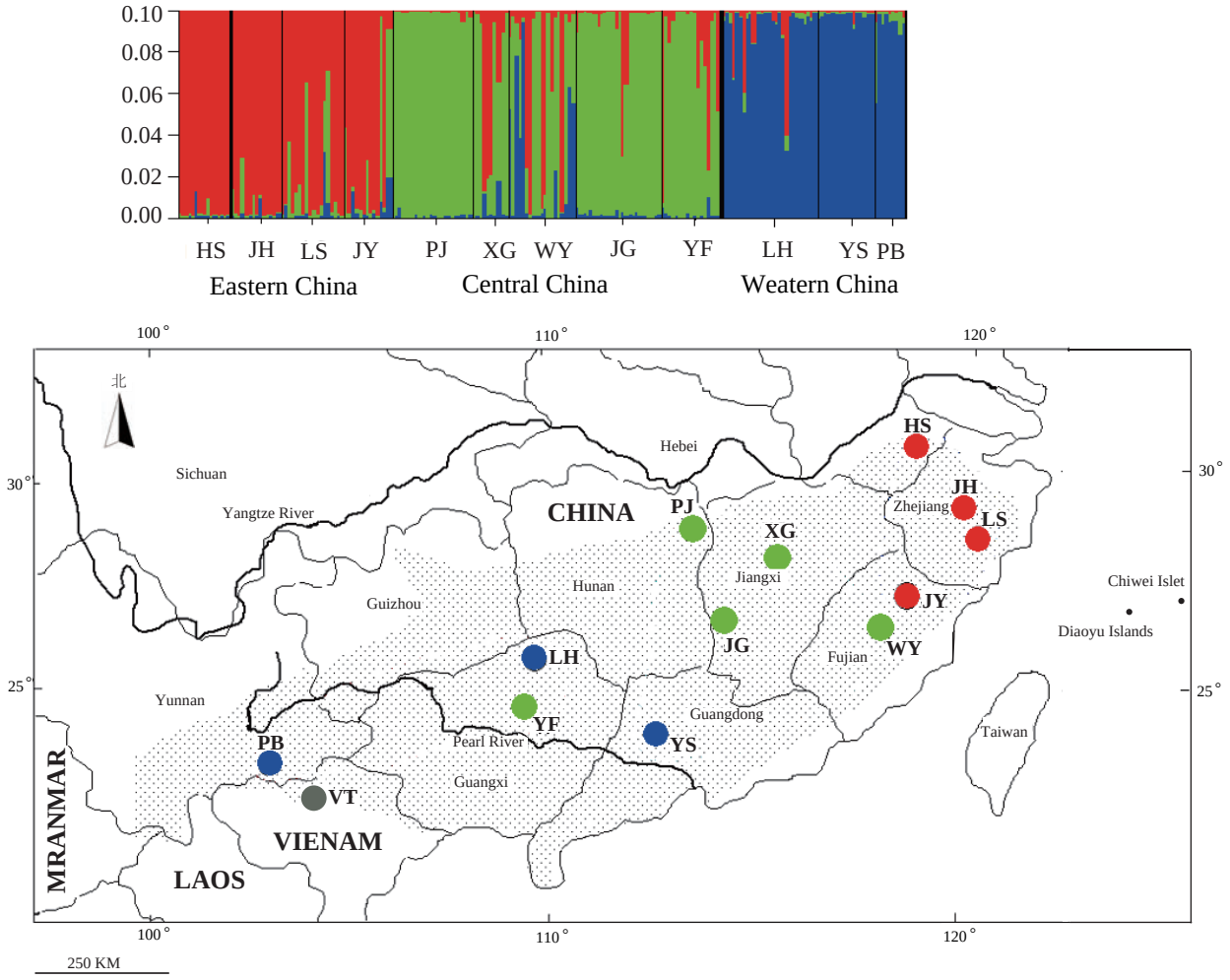

Figure 1 Color scheme: Bayesian cluster analysis of the microsatellite variation among the 12 giant spiny frog populations. Each vertical line represents an individual. The color composition displays the probability of belonging to each of the three clusters as defined by STRUCTURE. The three colors (red, blue, and green) represent the three genetic clusters. Map: Map of sampling localities for this study. The 13 sampled localities have colors corresponding to the genetic cluster wherein the majority of their respective individuals were assigned. Table 1 shows the abbreviation and coordinates of localities. The dotted area shows the distribution of giant spiny frog.

These sites defined a total of 51 haplotypes (Figure 2). The haplotypic sequences were deposited in GenBank with accession Nos. EU156068–156118. Each population has two to seven haplotypes. Each population also contained unique haplotypes.

Haplotype and nucleotide diversities were respectively h=0.968±0.006 and π=0.1152±0.0068 for all samples combined. The nucleotide diversity had an overall trend of decline from west to east (Table 4). Estimates of sequence divergence (K2P) among populations ranged from 0.419% (Jianyang, Fujian Province vs. Longsheng, Guangdong Province) to 24.37% (Northern Vietnam vs. Wuyishan, Fujian Province) (Table S4).

Phylogenetic relationship and population structure: The ML and Bayesian inference produced highly similar topologies, which clustered the haplotypes into four major clades, i.e., Northern Vietnam, Western China, Central China, and Eastern China clades (Figure 2). The clade names refer to their geographical pattern. The Northern Vietnam clade has three unique haplotypes, which formed the most basal branch in all phylogenetic reconstructions. Haplotypes H39 and H41 were shared in the Central and Eastern China clades despite having a closer relationship with other haplotypes of the Eastern China clade. Genetic distances among four major clades (range: 7.121–20.027) were almost one order of magnitude higher than those within each group (range: 0.925–8.671; Table 4). To provide a statistical evaluation of the geographical patterns suggested by the phylogenies, all possible sets of AMOVA comparisons were calculated. In the schemes dividing the giant spiny frog populations into two, three,

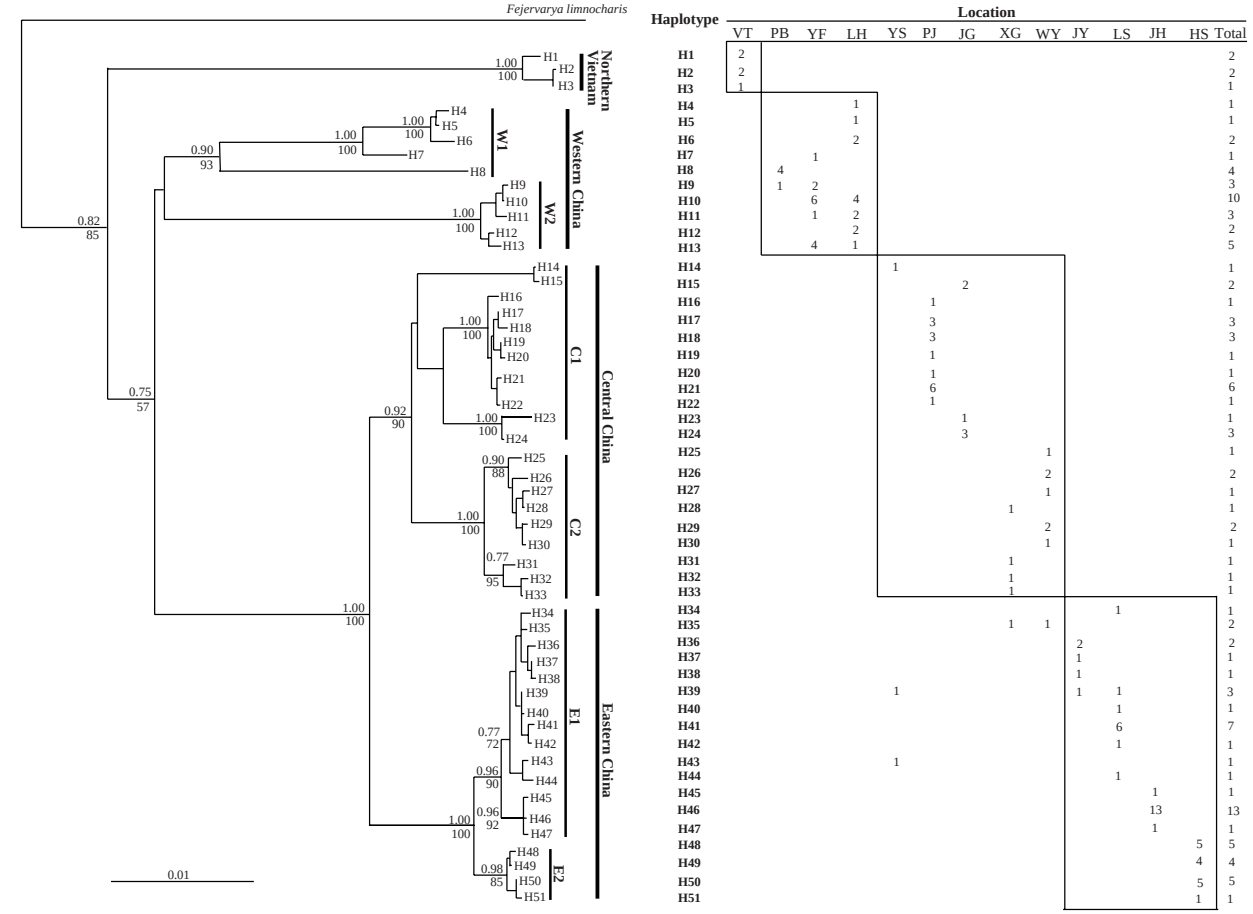

Figure 2 Phylogenetic relationships of haplotypes, and geographic distribution and frequency of each haplotype in the giant spiny frog. Phylogenetic relationships of haplotypes based on the Cyt *b* gene sequences were derived from Maximum-likelihood (GTR+I+G model) algorithm and Bayesian inference. The numbers above and below the branches are bootstraps and posterior probabilities values, which only shows values higher than 50%. *Fejervarya limnocharis* was the outgroup species for rooting the tree.

four, and five groups, the grouping scheme of four groups had a high Φ_{CT} value (Φ_{CT} = 0.0715, $P < 0.01$; Table S5). Genetic distances among the four major clades of giant spiny frogs ranged from 7.12% (Eastern China clade vs. Central China clade) to 20.03% (Northern Vietnam clade *vs.* Central China clade) (Table 5).

Diagnostic sites: Figure S1 shows the 30 diagnostic sites that clearly distinguished the four major clades. The special base composition at sites 41, 164, 458, and 463 differentiated the alleles H34–51 from the Eastern China clade with all alleles from other three major clades, and the "C" at site 98 only occurred in the haplotypes from the Central China clade (Figure S1). Diagnostic sites were also found between certain subclades, e.g., subclade W1 *vs.* subclade W2 and subclade E1 *vs.* subclade E2 (Figure S1).

4. Discussion

4.1 Genetic diversity within *Q. spinosa* This study is the first to analyze the genetic diversity and structure of wild giant spiny frog populations using a multiplex set of microsatellite markers. Our result showed that the *PIC* of the majority of the markers was high (92%, range: 0.23–0.94), which indicated that the 10 microsatellite markers were highly polymorphic and can thus be used for genetic diversity and population structure analyses of giant spiny frog (Botstein *et al.*, 1980). The average allele number of the 10 loci in giant spiny frog was 33.9/locus, which is significantly higher than the average allele number in some Anura species (Andersen *et al.*, 2004; Burns *et al.*, 2004). The allele number is usually positively associated with sample size (Goldstein *et al.*, 2005). However, the high polymorphism of the 10 microsatellites enabled

Table 4 The haplotype diversity (h) and nucleotide diversities (π) of Cyt *b* gene in each population of giant spiny frog.

Location	h	π
Northern Vietnam (VT)	0.800±0.164	0.00925±0.00248
Pingbian (PB)	0.400±0.237	0.09181±0.05447
Yongfu (YF)	0.758±0.084	0.02951±0.01893
Longsheng (LH)	0.848±0.074	0.09005±0.01829
Yangshan (YS)	1.000±0.126	0.09401±0.03056
Pingjiang (PJ)	0.825±0.071	0.00340±0.00058
Jinggangshan (JG)	0.905±0.103	0.09929±0.02933
Xingan (XG)	1.000±0.126	0.04057±0.01753
Wuyishan (WY)	0.750±0.063	0.02440±0.01413
Jianyang (JY)	0.800±0.164	0.00321±0.00069
Lishui (LS)	0.727±0.144	0.00285±0.00100
Jinhua (JH)	0.257±0.142	0.00047±0.00027
Huangshan (HS)	0.752±0.056	0.00275±0.00026
Total	0.968±0.006	0.11520±0.00680

the researchers to use powerful statistical tools to analyze genetic diversity and population structure in 12 populations. HWE is an important prerequisite for population genetic analysis, but the observed allele frequency in more than 50% of the loci in each population was found significantly deviate from HWE in some studies (Musammilu *et al.*, 2014; Zhou *et al.*, 2004). The significant deviation is generally caused by insufficient sample size, null alleles, loss of random mating, and the Wahlund effect (Rousset and Raymond, 1995; Wahlund, 1928; You *et al.*, 2008). AMOVA of microsatellites also revealed that variation among populations was 1.59%. Therefore, the Wahlund effect can be excluded because of low genetic differentiation among populations. We detected null alleles in four loci (Psp6, Psp9, Psp10, and Psp14). However, low frequencies (0.08–0.15) of null alleles cannot result in genetic disequilibrium. Non-amplifying samples in repeated trials were not present in any of the primer pairs in the 12 populations of *Q. spinosa*. The deviation of the loci in this study may be attributed to the relatively small sample size and heterozygote deficiencies, which are caused by selection, population mixing, or nonrandom mating (Rousset and Raymond, 1995).

As shown by the significant departure from HWE at some microsatellite loci, the observed heterozygosities were relatively low in all populations (Table S2). A heterozygote deficit is likely to be apparent in *Q. spinosa* from the 12 populations, and heterozygosity might be more vulnerable to selection pressures and/or habitat changes (Musammilu *et al.*, 2014). No historical data were available on the genetic diversity and heterozygosity of *Q. spinosa* but departure of the microsatellite data from HWE expectation in all populations may be attributed to commercial over-exploitation and habitat destruction. Although *Q. spinosa* is listed as vulnerable by the IUCN and the China Red List (Lau *et al.*, 2004; Zhao, 1998), many populations accessible to hunters may already have been extirpated because such populations may be hunted multiple times per year by multiple hunters (Chan *et al.*, 2014).

Despite using a similar method of analysis, the mean H_O levels found in this study (0.49–0.72) are higher than those found by Andersen *et al*. (2004) for the Danish European tree frog populations (0.35–0.53) and by Newman and Squire (Newman and Squire, 2001) for the common and widespread *Rana sylvatica* (0.44–0.50). However, this results of this study are similar to those on the formerly widespread *Litoria aurea* (0.43–0.82) by Burns *et al*. (2004). Higher genetic variation in wild giant spiny frog populations can positively affect the protection of giant spiny frog.

Table 5 Pairwise genetic distances for Cyt *b* sequences of the giant spiny frog. Below diagonal: Net genetic distances between the four major phylogenetic clades [PiXY–(PiX+PiY)/2]. Above diagonal: their standard errors of distances between the four major phylogenetic clades. Values within clades and their standard errors in parenthesis are shown in the diagonal (PiX).

	Northern Vietnam	Western China	Central China	Eastern China
Northern Vietnam	0.925(0.248)	2.441	2.267	2.266
Western China	17.245	8.671(1.384)	1.134	1.421
Central China	20.027	13.523	5.186(1.029)	0.651
Eastern China	18.451	14.176	7.121	1.566(0.078)

4.2 Phylogeography and population structure Amphibians, especially frogs, have species recognition and mate choice systems that rely on non-morphological characteristics (e.g. advertisement calls) and have the tendency to exhibit conservative morphological evolution. Thus, frogs are considered to have a large amount of cryptic genetic diversity (Bickford *et al.*, 2007; Funk *et al.*, 2012; Stuart *et al.*, 2006). In the Vietnam population, the microsatellite loci were either non-amplifying (Vietnam) or have a high number of private alleles in clades (Table S3). Differentiation at microsatellite loci among clades can indirectly support reproductive isolation. *Q. spinosa* exhibits high site fidelity, with some individuals found in similar locations in successive years (Chan *et al.*, 2014; Palo *et al.*, 2004). The microsatellite dataset on the 12 giant spiny frog populations (except Vietnam) exhibited a moderate or large genetic differentiation with an overall F_{ST} of 0.1057, which was expected for the frog with low dispersal rates. *Q. spinosa* is thus expected to exhibit a higher degree of population subdivision than any other major animal taxa because of poor dispersal capabilities (Chan *et al.*, 2014; Palo *et al.*, 2004). STRUCTURE suggested that the frog populations can be split into three distinct genetic clusters, i.e., Western China, Central China, and Eastern China, respectively (Figure 2). Although AMOVA only explained 1.95% of the observed genetic variation among groups, it was statistically significant (P<0.001). The genetic variation confirmed the existence of differentiation among the three groups. The phylogenetic trees using Cyt *b* gene further corroborated that the four clades are evolutionarily distinct (Figure 2). Relationships among the samples from different geographical locations and putative phylogeographic groups using microsatellite and mitochondrial markers were congruent with the results of Ye *et al*. (2013).

The clustering result matched the geographic distribution and geological topography of the populations. Giant spiny frogs distributed in the eastern areas are isolated from the frogs in central regions by strong biogeographic barriers, such as Poyang Lake, Gan River, and Wuyi Mountains. The phylogenetic reconstructions based on Cyt *b* gene also generated a topology that showed a stepwise-ladder pattern (Figure 2). Out of the four clades, the Northern Vietnam clade was the most basal branch, followed by the divergence of Western China clade and the Central and Eastern China clades. The west-to-east dispersal can also be corroborated by the gradual decrease in genetic diversity from west to east. Populations from the original location generally usually lose their genetic diversities during dispersal or expansion (e.g., Yang *et al*., 2004).

The large number of variable sites (38.79%) and parsimony-informative sites (37.54%) in Cyt *b* gene also proved that *Q. spinosa* may be a species complex. Genetic distances among the four major clades of giant spiny frogs are higher than or comparable with those reported in previous studies (Barber, 1999; Bradley Shaffer *et al.*, 2004; Elmer *et al.*, 2007; Yu *et al.*, 2015), as shown by interspecific differentiation in most other frogs. Barber (1999) found mean pairwise distances ranging from 12% to 20% for mitochondrial Cyt *b* sequences among different *Hyla* species (i.e., *H. arenicolor* and *H. eximia*), which are comparable with the divergences among the four major clades in this study. Some diagnostic sites and unique alleles were also found to distinguish each subclade pair reliably (Figure S1; Table S3).

However, STRUCTURE showed that the YF and YS populations were respectively clustered to the Central and Western China clades. This result differed from those of mitochondrial analysis (Figure 1). Admixture structure also existed in some populations, i.e., YF population mixed with the cluster of Eastern China despite being near the cluster of Western China according to geographical distance. The XG and WY populations also mixed among the three clusters (Figure 1). Discordance between mtDNA and nDNA genes can be attributed to introgression between distinct groups, differences between male and female dispersal rates, or incomplete lineage sorting of ancestral polymorphism (Qu *et al.*, 2012; Yang and Kenagy, 2009).

Our data rejected the possibility that introgression caused the pattern. Introgression always occurred in contact-zone individuals (Yang and Kenagy, 2009). However, admixture was found among far-distance populations, i.e., XG and WY populations showed a mixing among three clusters. Another three populations from Central China only mixed with the cluster of Eastern China. The population of Western China (e.g., LH) mixed with the cluster of Eastern China. As an alternative, we considered that the retention of ancestral polymorphism at the nuclear microsatellite loci likely caused the mixing. The uniparental inheritance of mtDNA resulted in an effective population size four times smaller than that of bi-parentally inherited nuclear DNA. Thus, nuclear DNA is more likely to retain ancestral polymorphism (Yang and Kenagy, 2009). However, further systematic sampling from more areas and more molecular markers should be used in future investigations to confirm the present hypothesis.

4.3 Implications for conservation Our research coupled with other studies suggests that *Q. spinosa* might be a species complex (Che *et al.*, 2009; Ye *et al.*, 2013). The failure to diagnose biological diversity can hamper conservation efforts and basic scientific inquiry (Mayden and Wood, 1995). Conservation decisions are often made on the assumption that named taxonomic units represent evolutionary lineages. Phylogeographic analysis provides valuable information on how intraspecific genetic variation is partitioned. Such analysis also identifies evolutionary significant units (ESUs) and management units (MUs) for species. According to the criterion proposed by Moritz (1994), populations that are differentiated for mtDNA haplotypes or at nuclear loci are designated as MUs, whereas those that are reciprocally monophyletic for mtDNA haplotypes and show significant differentiation at nuclear loci are given ESU status. The molecular data presented in this work indicate significant geographical structuring of genetic variation across the range of *Q. spinosa*, and the topologies of all phylogenetic trees derived from all sequences (Figure 2) showed that reciprocal monophyly criterion for ESU designation was met by the Northern Vietnam, Western China, Central China, and Eastern China clades.

A precise and correct delimitation of species is essential because species are basic units for analysis in biogeography, ecology, macroevolution, biodiversity assessment, and conservation and management (Francesca *et al.*, 2006; Sites Jr and Marshall, 2004). Over- or under-resolving species boundaries can result in erroneous decisions for management and conservation (Francesca *et al.*, 2006; Sites Jr and Marshall, 2004). This suggests that a re-evaluation of *Q. spinosa* boundaries and conservation status is needed. Our results show that *Q. spinosa* can be divided into multiple ESUs and all of them should be considered as evolutionary independent units, and hence should be independently managed wherever possible to avoid the break-up of coadapted gene complexes and other forms of outbreeding depression (Tallmon *et al.*, 2004; Ficetola and De Bernardi, 2005; Ficetola *et al.*, 2007). At present, most frog farms are using *Q. spinosa* from different geographical populations, which will lead to a risk of genetic contamination and a threat of pathogen transmission. So, it is necessary to make periodic genetic evaluations of the source population to ensure that they are genetically similar (Borrell *et al.*, 2011).

To protect the relatively abundant genetic variations held in different clades, the four phylogenetic clades and some subclades with distinct geographic distribution may be regarded as independent management units for conservation purposes.

Acknowledgements We are debit to many people who have helped us in collecting samples for this study, in particular Chuntao LIU, Canyang LI, and Xinsheng TANG (Huangshan University). We also want to thank Jiayong ZHANG and Lian CHEN for their assistance in the laboratory work. This research was supported by the National Science Foundation of China (No. 31172116 and No. 31472015), by the Major Science and Technology Specific Projects of Zhejiang Province of China (No. 2010C12008), by the project of the Science Technology Commission of Zhejiang Province of China (No. 2011C22006), by the Found for the science and technology innovation team of Zhejiang Province of China (No. 2012R10026-07), and by the Key Program of the Twelfth Five Year New Aquatic Varieties Breeding Cooperation of Zhejiang Province of China (2012C12907-9)

References

Andersen L. W., Fog K., Damgaard C. 2004. Habitat fragmentation causes bottlenecks and inbreeding in the European tree frog (*Hyla arborea*). Proc R Soc Lond B Biol Sci, 271: 1293–1302

Barber P. 1999. Phylogeography of the canyon treefrog, *Hyla arenicolor* (Cope) based on mitochondrial DNA sequence data. Mol Ecol, 8: 547–562

Bickford D., Lohman D. J., Sodhi N. S., Ng P. K., Meier R., Winker K., Ingram K. K., Das I. 2007. Cryptic species as a window on diversity and conservation. Trends Ecol Evol, 22: 148–155

Borrell Y. J., Alvarez J., Blanco G., de Murguía A. M., Lee D., Fernández C., Martínez C., Cotano U., Álvarez P., Prado J. A. S. 2011. A parentage study using microsatellite loci in a pilot project for aquaculture of the European anchovy *Engraulis encrasicolus* L. Aquaculture, 310: 305–311

Bossuyt F., Milinkovitch M. C. 2000. Convergent adaptive radiations in Madagascan and Asian ranid frogs reveal covariation between larval and adult traits. Proc Natl Acad Sci, 97: 6585–6590

Botstein D., White R. L., Skolnick M., Davis R. W. 1980. Construction of a genetic linkage map in man using restriction fragment length polymorphisms. Am J Hum Genet, 32: 314–331

Bradley S. H., Fellers G. M., Randal V. S., Oliver J. C., Pauly G. B. 2004. Species boundaries, phylogeography and conservation genetics of the red-legged frog (*Rana aurora/draytonii*) complex. Mol Ecol, 13: 2667–2677

Burns E. L., Eldridge M. D., Houlden B. A. 2004. Microsatellite variation and population structure in a declining Australian Hylid *Litoria aurea*. Mol Ecol, 13: 1745–1757

Chan H. K., Shoemaker K. T., Karraker N. E. 2014. Demography of *Quasipaa* frogs in China reveals high vulnerability to widespread harvest pressure. Biol Conserv, 170: 3–9

Che J., Hu J. S., Zhou W. W., Murphy R. W., Papenfuss T. J., Chen M. Y., Rao D. Q., Li P. P., Zhang Y. P. 2009. Phylogeny of the Asian spiny frog tribe Paini (Family Dicroglossidae) sensu Dubois. Mol Phyl Evol, 50: 59–73

Du J., Yan J., Zhou K. 2012. Isolation of microsatellite markers for *Pelophylax nigromaculata* and a tentative application in detecting interspecific introgression. Gene, 508: 130–134

Dupuis J. R., Roe A. D., Sperling F. A. 2012. Multi-locus species delimitation in closely related animals and fungi: one marker is not enough. Mol Ecol, 21: 4422–4436

Elmer K. R., Dávila J. A., Lougheed S. C. 2007. Cryptic diversity and deep divergence in an upper Amazonian leaflitter frog, *Eleutherodactylus ockendeni*. BMC Evol Biol, 7: 247

Evanno G., Regnaut S., Goudet J. 2005. Detecting the number of clusters of individuals using the software STRUCTURE: a simulation study. Mol Ecol, 14: 2611–2620

Ficetola G. F., De Bernardi F. 2005. Supplementation or in situ conservation? Evidence of local adaptation in the Italian agile frog *Rana latastei* and consequences for the management of populations. Anim Conserv, 8: 33–40

Ficetola G. F., Garner T., De Bernardi F. 2007. Genetic diversity, but not hatching success, is jointly affected by postglacial colonization and isolation in the threatened frog, *Rana latastei*. Mol Ecol, 16: 1787–1797

Francesca Z., Roberta C., Giuseppe N. 2006. Genetic relationships of the western Mediterranean painted frogs based on allozymes and mitochondrial markers: evolutionary and taxonomic inferences (Amphibia, Anura, Discoglossidae). Biol J Linn Soc, 87: 515–536

Frost D. R., Grant T., Faivovich J., Bain R. H., Haas A., Haddad C. F. B., De Sá R. O., Channing A., Wilkinson M., Donnellan S. C., Raxworthy C. J., Campbell J. A., Blotto B. L., Moler P., Drewes R. C., Nussbaum R. A., Lynch J. D., Green D. M., Wheeler W. C. 2006. The amphibian tree of life. Bull Am Mus Nat Hist, 297: 1–370.

Funk W. C., Caminer M., Ron S. R. 2012. High levels of cryptic species diversity uncovered in Amazonian frogs. Proc R Soc B, 279: 1806–1814

Goldstein P., Wyner Y., Doukakis P., Egan M. G., Amato G., Rosenbaum H., DeSalle R. 2005. Theory and methods for diagnosing species and populations in conservation. Ann Miss Bot Gard, 92: 12–27

Guo S. W., Thompson E. A. 1992. Performing the exact test of Hardy–Weinberg proportion for multiple alleles. Biometrics, 48: 361–372

Huelsenbeck J. P., Ronquist F. 2001. Mrbayes: Bayesian inference of phylogenetic trees. Bioinformatics, 17: 754–755

Lau M. W. N., Geng B., Gu H., van Dijk P. P., Bain R. 2004. *Quasipaa spinosa*, in: IUCN 2012. IUCN Red List of Threatened Species. Version 2012.1. www.iucnredlist.org

Lewis P. O., Zaykin D. 2000. Genetic Data Analysis: computer program for the analysis of allelic data. Version 1.0 (d15). Available at http://hydrodictyon. eeb.uconn.edu/people/plewis/software.php

Liang Z., Xu Q., Jiang Y., Qin J., Deng W. 2013. Situation and development of Quasipaa spinosa in Yongfu County. Guangxi Anim. Husbandry Veterinary Med, 29: 244–246 (in Chinese)

Liu Z. Q., Wang Y. Q., Su B. 2005. The mitochondrial genome organization of the rice frog, *Fejervarya limnocharis* (Amphibia: Anura): a new gene order in the vertebrate mtDNA. Gene, 346: 145–151

Marshall T. C., Slate J., Kruuk L. E. B., Pemberton J. M. 1998. Statistical confidence for likelihood-based paternity inference in natural populations. Mol Ecol, 7: 639–655

Mayden R. L., Wood R. M. 1995. Systematics species concepts and the evolutionarily significant unit in biodiversity and conservation biology. Am Fisheries Soc Symp, 17: 58–113

Miller P. A., Fitch A. J., Gardner M., Hutson K. S., Mair G. 2011. Genetic population structure of Yellowtail Kingfish (*Seriola lalandi*) in temperate Australasian waters inferred from microsatellite markers and mitochondrial DNA. Aquaculture, 319: 328–336

Moritz C. 1994. Applications of mitochondrial DNA analysis in conservation: a critical review. Mol Ecol, 3: 401–411

Musammilu K., Abdul-Muneer P., Gopalakrishnan A., Basheer V., Gupta H., Mohindra V., Lal K. K., Ponniah A. 2014. Identification and characterization of microsatellite markers for the population genetic structure in endemic red-tailed barb, *Gonoproktopterus curmuca*. Mol Boil Rep, 41: 3051–3062

Newman R. A., Squire T. 2001. Microsatellite variation and fine-scale population structure in the wood frog (*Rana sylvatica*). Mol Ecol, 10: 1087–1100

Palo J. U., Schmeller D. S., Laurila A., Primmer C. R., Kuzmin S. L., Merilä J. 2004. High degree of population subdivision in a widespread amphibian. Mol Ecol, 13: 2631–2644

Posada D., Crandall K. A. 1998. Modeltest: testing the model of DNA substitution. Bioinformatics, 14: 817–818

Pritchard J. K., Stephens M., Donnelly P. 2000. Inference of population structure using multilocus genotype data. Genetics, 155: 945–959

Qu Y., Zhang R., Quan Q., Song G., Li S. H., Lei F. 2012. Incomplete lineage sorting or secondary admixture: disentangling historical divergence from recent gene flow in the Vinous-throated parrotbill (*Paradoxornis webbianus*). Mol Ecol, 21:6117–6133

Rousset F., Raymond M. 1995. Testing heterozygote excess and deficiency. Genetics, 140: 1413–1419

Rozas J., Sánchez-DelBarrio J. C., Messeguer X., Rozas R. 2003. DnaSP, DNA polymorphism analyses by the coalescent and other methods. Bioinformatics, 19: 2496–2497

Sambrook J., Fritsh E. F., Maniatis T. 1989. Molecular Cloning: a Laboratory Manual, second edition. New York, England: Cold Spring Harbor Laboratory Press

Schneider S., Roessli D., Excoffier L. 2000. Arlequin Ver. 2.001: a Software for Population Genetic Data Analysis. Genetics and Biometry Laboratory, Department of Anthropology, University of Geneva, Switzerland

Schuelke M. 2000. An economic method for the fluorescent labeling of PCR fragments. Nat Biotechnol, 18: 233–234

Simon C., Frati F., Beckenbach A., Crespi B., Liu H., Flook P. 1994. Evolution, weighting, and phylogenetic utility of mitochondrial gene sequences and a compilation of conserved polymerase chain reaction primers. Ann Entomol Soc Am, 87: 651–701

Sites Jr J. W., Marshall J. C. 2004. Operational criteria for delimiting species. Ann Rev Ecol Syst, 35: 199–227

Stuart B. L., Inger R. F., Voris H. K., 2006. High level of cryptic species diversity revealed by sympatric lineages of Southeast Asian forest frogs. Biol Lett, 2: 470–474

Stuart S. N., Chanson J. S., Cox N. A., Young B. E., Rodrigues A. S., Fischman D. L., Waller R. W. 2004. Status and trends of amphibian declines and extinctions worldwide. Science, 306: 1783–1786

Swofford D. L. 2002. PAUP*: phylogenetic analysis using parsimony, Version 4. Sinauer Associates, Sunderland, Massachusetts

Tallmon D. A., Luikart G., Waples R. S. 2004. The alluring simplicity and complex reality of genetic rescue. Trends Ecol Evol, 19: 489–496

Tamura K., Dudley J., Nei M., Kumar S. 2007. MEGA4: molecular evolutionary genetics analysis (MEGA) software version 4.0. Mol Biol Evol, 24: 1596–1599

Tamura K., Peterson D., Peterson N., Stecher G., Nei M., Kumar S. 2011. MEGA5: molecular evolutionary genetics analysis using maximum likelihood, evolutionary distance, and maximum parsimony methods. Mol Boil Evol, 28: 2731–2739

Thompson J. D., Gibson T. J., Plewniak F., Jeanmougin F., Higgins D. G. 1997. The CLUSTAL_X windows interface: flexible strategies for multiple sequence alignment aided by quality analysis tools. Nuc Acid Res, 25: 4876–4882

Wahlund S. 1928. Zusammensetzung von populationen und korrelationserscheinungen vom standpunkt der vererbungslehre aus betrachtet. Hereditas, 11: 65–106

Weir B. S., Cockerham C. C. 1984. Estimating F-statistics for the analysis of population structure. Evolution, 38: 1358–1370

Wright S. 1978. Evolution and the genetics of populations. Chicago, America: University of Chicago Press

Xie F., Lau M. W. N., Stuart S. N., Chanson J. S., Cox N. A., Fischman D. L. 2007. Conservation needs of amphibians in China: A review. Sci China C, 50: 265–276

Yang D. S., Kenagy G. J. 2009. Nuclear and mitochondrial DNA reveal contrasting evolutionary processes in populations of deer mice (*Peromyscus maniculatus*). Mol Ecol, 18: 5115–5125

Yang Y. H., Zhang D. X., Li Y. M., Ji Y. J. 2004. Mitochondrial DNA diversity and preliminary biogeography inference of the evolutionary history of the black-spotted pond frog *Rana nigromaculata* populations in China. Acta Zool Sin, 50: 193–201

Ye C., Fei L., Hu S. 1993. Rare and economic amphibians of China. Chengdu, China: Sichuan Publishing House of Science and Technology (in Chinese)

Ye S. P., Huang H., Zheng R. Q., Zhang J. Y., Yang G., Xu S. X. 2013. Phylogeographic Analyses Strongly Suggest Cryptic Speciation in the Giant Spiny Frog (Dicroglossidae: *Paa spinosa*) and Interspecies Hybridization in *Paa*. PloS one, 8:e70403

You E. M., Chiu T. S., Liu K. F., Tassanakajon A., Klinbunga S., Triwitayakorn K., de La Peña L. D., Li Y., Yu H. T. 2008. Microsatellite and mitochondrial haplotype diversity reveals population differentiation in the tiger shrimp (*Penaeus monodon*) in the Indo-Pacific region. Anim Genet, 39: 267–277

Yu B. G., Zheng R. Q., Zhang Y., Liu C. T. 2010. Geographic variation in body size and sexual size dimorphism in the giant-spiny frog *Paa spinosa* (David, 1875) (Anura: Ranoidae). J Nat Hist, 44: 1729–1741

Yu D. N., Zhang J. Y., Peng L., Shao C., Zheng R. Q. 2015. Do cryptic species exist in *Hoplobatrachus rugulosus*? An examination using four nuclear genes, the Cyt b Gene and the complete mt genome. PLoS One 10: e0124825

Zhao E. M. 1998. China Red Data Book of Endangered Animals-Amphibia. Beijing, China: Science Press (in Chinese).

Zheng R. Q., Ye R. H., Yu Y. Y., Yang G. 2009. Fifteen polymorphic microsatellite markers for the giant spiny frog, *Paa spinosa*. Mol Ecol Resour, 9: 336–338

Zhou J., Wu Q., Wang Z., Ye Y. 2004. Genetic variation analysis within and among six varieties of common carp (*Cyprinus carpio L.*) in China using microsatellite markers. Russ J Genet (Genet), 40: 1144–1148

Supplementary Data

Table S1 Characteristics of the ten polymorphic microsatellite loci isolated from the giant spiny frog.

Locus	Repeat Motif	Primer Sequences (5′—3′)	Size range (bp)	*T*a (°C)	Source
Psp1	$(GT)_{18}$	F: 5′-CATTGGCACTGCTGTTATCC-3′ R: 5′-GACCTGTGACAGCTTCTTTGTG-3′	213–243	59	Zheng *et al.* (2009)
Psp2	$(GT)_7T(TG)_6$	F: 5′-AACAGTGAAAGAACCGAAAC-3′ R: 5′-CCCACAATGGAATGGACACG-3′	142–178	51.5	Zheng *et al.* (2009)
Psp6	$(GT)_{12}…(GT)_6A$ T$(GT)_6$	F: 5′-CACGCAAAGTGAAACGCT-3′ R: 5′-CTCCCCAACGACACACG-3′	291–351	65	Zheng *et al.* (2009)
Psp7	$(GT)_{13}$	F: 5′-ACTCTACAGCAAGTAAAAGC-3′ R: 5′ –CCCAAAATCAGAAAATAAT-3′	161 – 173	52.5	Zheng *et al.* (2009)
Psp8	$(CA)_{12}$	F: 5′- TGCTTGGTAGTTTGCGATT-3′ R: 5′- CGTGACCGGAGTGATGTC-3′	314–358	62	Zheng *et al.* (2009)
Psp9	$(AC)_7$	F: 5′-GGATCAGCAAGCAACATTAT-3′ R: 5′-CAGTCCCAGTTTCTTCTCAC-3′	220–236	49	Zheng *et al.* (2009)
Psp10	$(CG)_9(CA)_{48}$	F: 5′- AAAACACAAACAAAAGAA-3′ R: 5′- AACAGGGTAAATATGGAC-3′	272–364	55	Zheng *et al.* (2009)
Psp11	$(GT)_{18}$	F: 5′-GGACAGGGTGAAGGCAGTAT-3′ R: 5′-CCTGTGAGGCAATATGAAAA-3′	224–274	55.5	Zheng *et al.* (2009)
Psp12	$(GT)_{27}$	F: 5′-TTAAAATAGCCAACCAG-3′ R: 5′-CATCAATTACCACATGC-3′	234–286	50	Zheng *et al.* (2009)
Psp14	(TG)11	F: 5′-ATGGCTGGTGGAAAAAGACT-3′ R: 5′-TAGGAGGGGCAACGGAG-3′	228–300	59	Zheng *et al.* (2009)

Table S2 Allele number (*N*a), observed (*H*o) and expected (*H*e) heterozygosity and polymorphic information content (*PIC*) in the twelve populations of giant spiny frog.

Pop	Parameters	Loci										
		Psp8	Psp6	Psp7	Psp2	Psp9	Psp14	Psp10	Psp1	Psp12	Psp11	Mean
HS	Na	2	6	10	11	8	7	6	6	5	2	6.3
	Ho	0.00	0.29*	0.60*	0.73	0.87	0.80	0.93	0.47	0.27	1.00*	0.6
	He	0.27	0.69	0.87	0.88	0.83	0.75	0.79	0.77	0.54	0.52	0.69
	PIC	0.23	0.62	0.82	0.84	0.78	0.70	0.73	0.71	0.49	0.38	0.63
JH	Na	6	10	4	4	5	9	6	9	7	3	6.3
	Ho	0.64*	0.57	0.29*	0.14*	0.43*	0.71	0.50	0.64	0.50	0.43	0.49
	He	0.72	0.84	0.55	0.56	0.62	0.85	0.81	0.89	0.78	0.46	0.71
	PIC	0.65	0.79	0.49	0.46	0.54	0.80	0.74	0.84	0.72	0.40	0.64
LS	Na	9	10	9	11	3	14	6	14	10	12	9.8
	Ho	0.78	0.28*	0.83	0.83	0.28*	0.78	0.44	0.67	0.61*	0.61	0.61
	He	0.76	0.88	0.80	0.85	0.56	0.92	0.66	0.88	0.86	0.79	0.8
	PIC	0.71	0.84	0.75	0.81	0.45	0.88	0.61	0.85	0.81	0.75	0.75
JY	Na	10	10	8	8	5	12	9	12	9	14	9.7
	Ho	0.85	0.38*	0.77	0.31	0.77	0.54*	0.69	0.62*	0.69	0.85	0.65
	He	0.89	0.87	0.73	0.53	0.74	0.90	0.85	0.90	0.88	0.94	0.82
	PIC	0.84	0.82	0.68	0.49	0.66	0.85	0.80	0.86	0.82	0.90	0.77
PJ	Na	7	17	9	6	3	19	18	14	10	15	11.8
	Ho	0.48	0.74	0.61	0.65	0.13*	0.87	0.57*	0.52*	0.57	0.43*	0.56
	He	0.53	0.94	0.70	0.70	0.57	0.94	0.94	0.92	0.85	0.84	0.79
	PIC	0.50	0.91	0.67	0.63	0.47	0.92	0.92	0.90	0.82	0.81	0.76
XG	Na	10	11	11	10	5	10	15	9	11	9	10.1
	Ho	0.80*	0.40*	1.00	0.50	0.60*	0.40*	0.70*	0.40*	0.70	0.50*	0.60
	He	0.92	0.94	0.89	0.89	0.76	0.93	0.97	0.91	0.91	0.89	0.90
	PIC	0.86	0.89	0.84	0.83	0.68	0.87	0.92	0.85	0.85	0.83	0.84
JG	Na	10	12	11	11	6	18	17	16	26	15	14.2
	Ho	0.58*	0.79	0.38*	0.54*	0.33	0.67	0.54*	0.63*	0.75*	0.83	0.60
	He	0.78	0.89	0.65	0.85	0.40	0.93	0.92	0.93	0.97	0.93	0.83
	PIC	0.75	0.86	0.61	0.81	0.37	0.91	0.90	0.90	0.94	0.90	0.80
WY	Na	15	14	15	11	7	18	18	17	17	19	15.1
	Ho	0.74	0.32*	0.63*	0.63	0.58	0.53*	0.53*	0.68	0.56*	0.58*	0.58
	He	0.89	0.88	0.90	0.91	0.83	0.95	0.95	0.94	0.92	0.94	0.91
	PIC	0.86	0.85	0.87	0.88	0.79	0.92	0.92	0.91	0.88	0.91	0.88
LH	Na	9	10	12	15	7	12	17	18	15	12	12.7
	Ho	0.93*	0.58*	0.85	0.56*	0.48	0.37*	0.56*	0.68*	0.41*	0.70	0.61
	He	0.75	0.90	0.84	0.92	0.56	0.87	0.90	0.93	0.91	0.83	0.84
	PIC	0.71	0.87	0.81	0.90	0.50	0.84	0.88	0.90	0.88	0.79	0.81
YF	Na	7	10	8	11	6	7	10	9	14	9	9.1
	Ho	1.00	0.69	0.81	0.75	0.38*	0.56	0.63	0.56*	0.56*	0.63*	0.66
	He	0.77	0.90	0.66	0.92	0.72	0.83	0.91	0.88	0.92	0.89	0.84
	PIC	0.71	0.86	0.62	0.88	0.66	0.77	0.87	0.83	0.88	0.85	0.79
YS	Na	14	12	10	9	4	13	16	14	19	10	12.1
	Ho	1.00	0.59	0.76	0.47*	0.59	0.76	0.76*	0.76*	0.76*	0.76	0.72
	He	0.88	0.80	0.84	0.79	0.64	0.90	0.94	0.93	0.96	0.90	0.86
	PIC	0.84	0.76	0.79	0.74	0.57	0.86	0.90	0.90	0.93	0.86	0.82
PB	Na	11	8	9	9	7	16	10	10	11	8	9.9
	Ho	0.71*	0.29*	0.64*	0.71	0.71	0.71*	0.79	0.57*	0.86	0.79	0.68
	He	0.92	0.87	0.88	0.83	0.65	0.96	0.86	0.90	0.91	0.85	0.86
	PIC	0.87	0.82	0.83	0.78	0.60	0.92	0.81	0.85	0.87	0.80	0.82

An asterisk (*) indicates the locus which showed deviation from Hardy-Weinberg equilibrium.

Table S3 Numbers of unique alleles at the ten microsatellite loci in the three giant spiny frog groups.

Clusters	Locus										Total
	Psp1	Psp2	Psp6	Psp7	Psp8	Psp9	Psp10	Psp11	Psp12	Psp14	
Eastern China	1	2	7	3	0	1	3	1	2	2	22
Central China	4	2	6	4	6	4	9	11	12	7	65
Western China	2	4	1	0	4	0	1	3	4	2	21

Table S4 Mean genetic distance between population (below diagonal) and within group divergences (on the diagonal) based on K2P model from Cyt *b* data in the giant spiny frog.

Population	HS	JH	LS	JY	WY	XG	JG	PJ	YS	LH	YF	PB	VT
HS	**0.00275**												
JH	0.02784	**0.00047**											
LS	0.02521	0.01365	**0.00285**										
JY	0.02568	0.01314	0.00419	**0.00321**									
WY	0.07873	0.07415	0.07462	0.07460	**0.02440**								
XG	0.07158	0.06705	0.06566	0.06633	0.03404	**0.04057**							
JG	0.10545	0.11199	0.11280	0.11418	0.09687	0.09707	**0.0839**						
PJ	0.07075	0.07745	0.07919	0.07934	0.05376	0.05173	0.07914	**0.00343**					
YS	0.08612	0.08153	0.07482	0.07712	0.11461	0.10964	0.12436	0.11826	**0.09151**				
LH	0.15887	0.14241	0.16236	0.16475	0.14945	0.14964	0.15391	0.14137	0.16424	**0.08005**			
YF	0.19388	0.19623	0.19530	0.19861	0.18755	0.18625	0.18259	0.18436	0.17875	0.07165	**0.02951**		
PB	0.19309	0.19645	0.19480	0.19763	0.18588	0.18583	0.17950	0.18543	0.17417	0.17977	0.17644	**0.07181**	
VT	0.21151	0.21679	0.21625	0.21691	0.24371	0.24007	0.22821	0.22698	0.21245	0.21969	0.21030	0.18424	**0.00925**

Table S5 Hierarchical analysis of AMOVA of the giant spiny frog from Cyt *b* data.

Groups	Among pops within groups Φ_{SC}	Within pops Φ_{ST}	Among groups Φ_{CT}	(%) Among groups	*P*
2 Groups [HS, JH, LS, JY, WY, XG, JG, PJ][YS, LH, YF, PB, VT]	0.0948	0.3905	0.0519*	5.19	0.0342
3 Groups [HS, JH, LS, JY, WY, XG, JG, PJ][YS, LH, YF, PB][VT]	0.0891	0.3405	0.0373	3.73	0.0752
4 Groups [HS, JH, LS, JY][WY, XG, JG, PJ, YS][LH, YF, PB][VT]	0.0870	0.3211	0.0715**	7.15	<0.01
5 Groups [HS, JH, LS, JY][WY, XG, JG, PJ][YS, LH, YF][PB][VT]	0.0769	0.3867	0.0437	4.37	0.0547

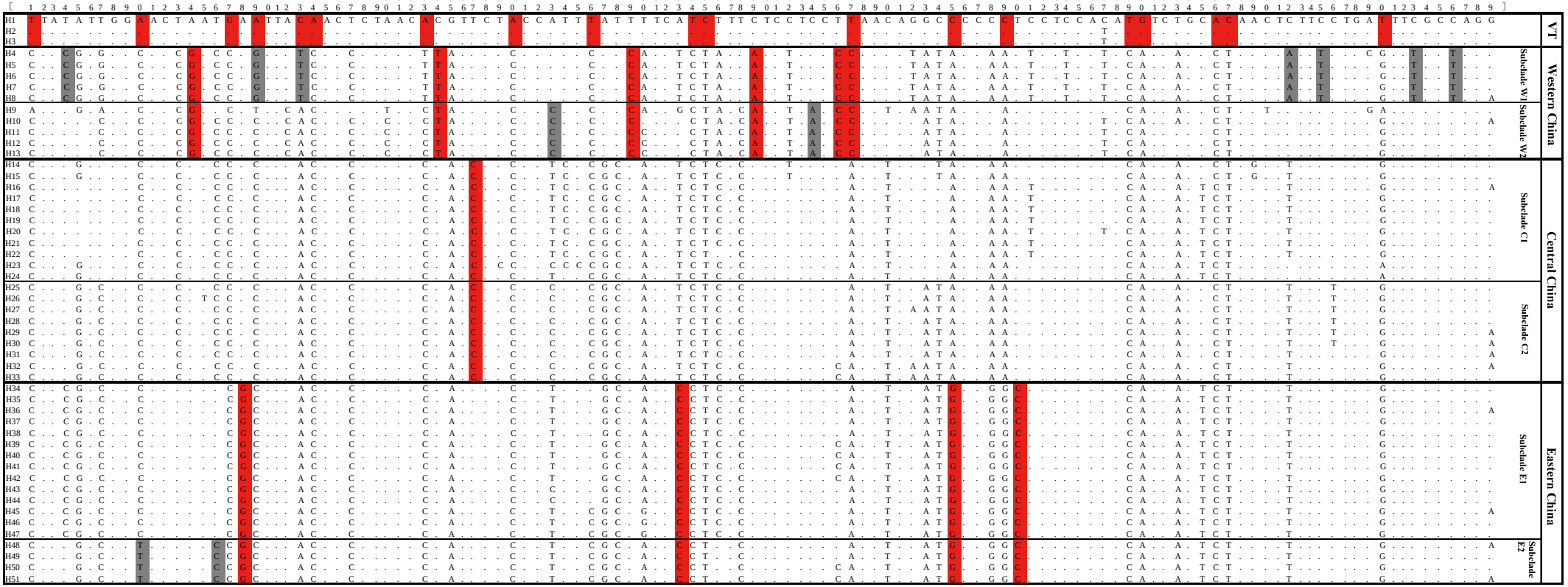

Figure S1 Variable sites in Cyt *b* fragment of the giant spiny frog, show the diagnostic sites. Numbers of haplotypes correspond to Figure 2. Red bars show the diagnostic sites distinguishing major clades. Grey bars show those can distinguish the sequences from subclades. VT, Northern Vietnam.